Icosahedral order in glass: Electronic properties

Michael Widom*

Department of Physics, Harvard University, Cambridge, Massachusetts 02138
(Received 17 December 1984)

Icosahedral short-range order in glass is modeled by a crystalline packing of atoms in S^3, known as polytope 120. We diagonalize realistic electronic Hamiltonians using the symmetry group of polytope 120. We predict band structures for amorphous semiconductors and transition metals. Icosahedral order in silicon produces a gap in the center of the valence band. The absence of d-level splitting at the center of the Brillouin zone distinguishes icosahedrally ordered transition metals from their fcc counterparts. We use the d-band density of states of polytope 120 to understand band ferromagnetism in amorphous transition metals.

INTRODUCTION

Frank and Kasper[1] based a theory of crystalline transition-metal alloys on the tendency of metal atoms to form icosahedral clusters. Crystalline order with icosahedral symmetry cannot[2] extend throughout $\mathbb{R}^3$. The Frank-Kasper phases consist of regions of icosahedral order interrupted by an ordered array of defect lines. Nelson[3] suggested that metallic glasses are Frank-Kasper phases in which the defect lines have become entangled.

Alternatively, we can think of metallic glass as infinite, densely packed[4] clusters of atoms. Hoare[5] observed that small dense clusters of atoms favor icosahedral coordination. Large clusters contain defects because $\mathbb{R}^3$ cannot be tiled with icosahedra. In S^3, however, we can build a 120-atom cluster in which each atom has icosahedral coordination. Coxeter[6] analyzed the resulting crystal, called polytope 120, in great detail. We describe the structure of polytope 120 in Sec. I.

Flat and curved spaces are indistinguishable at short distances. Thus we can construct clusters in $\mathbb{R}^3$ which become fragments of polytope 120 when projected into S^3. We hypothesize that metallic glass consists of regions of polytope 120 separated by regions of defects. Such a material could be called "microcrystalline." Microcrystalline materials usually consist of large domains of cubic order separated by grain boundaries, whereas our present model consists of relatively small domains of icosahedral order interrupted by disclination lines.

Kléman and Sadoc[7] and Sadoc and Mosseri[8,9] described a variety of polytopes related to polytope 120. Sadoc and Mosseri suggested that a configuration called polytope 240 could describe amorphous tetracoordinated semiconductors. Polytope 120 generates polytope 240 in the same way that the face-centered-cubic lattice generates the diamond lattice.

In order to test the relevance of polytopes to real glass, we calculate their electronic band structures. If glass consists of polytope microcrystals, some properties of the polytope should be observable in the bulk amorphous material. Nelson and Widom[10] showed rough agreement between the x-ray structure functions of the polytope and

metallic glass. Sachdev and Nelson[11] found improved agreement when they included the long-range disorder present in $\mathbb{R}^3$.

The situation should be similar in the electronic properties. We expect the best agreement in quantities which are more sensitive to the short-range order than to the long-range disorder. At low energies and long wavelengths,[10] the different topologies of $\mathbb{R}^3$ and S^3 lead to discrepancies in the electronic properties. We expect the best agreement in the energy range corresponding to wavelengths of the order of a few atomic diameters.

In the present paper, we compute the spectra of realistic tight-binding Hamiltonians on polytope 120 and polytope 240. We begin by constructing fragments of polytope 120 in $\mathbb{R}^3$ and describing the structure in S^3. A remarkable isomorphism exists between polytope 120 and $Y' \subset SU(2)$, the double group of an icosahedron. This isomorphism allows us to express the symmetry group, $G \subset SO(4)$, of the polytope in terms of the direct square of Y'. Many problems requiring the use of the symmetry group G of polytope 120 can be solved in terms of the symmetry group Y' of an icosahedron. We review the theory of representations of Y' and G.

Section II concerns the formal diagonalization of tight-binding Hamiltonians. In part A, we solve an s-band, nearest-neighbor, hopping model. Although this model has been discussed previously,[10,12] we present its solution here because we use the eigenfunctions to diagonalize more complicated and realistic models. We show indirect evidence for the existence of a reciprocal space for polytope 120.

In part B, we define a Weaire and Thorpe[13] Hamiltonian on polytope 240. This Hamiltonian describes the hopping of sp^3-hybrid electrons on a tetracoordinated lattice. Using methods of Thorpe and Weaire,[14] as extended by Straley,[15] we reduce this problem to the simple model considered in part A and obtain analytic expressions for the eigenvalues.

Finally, in part C, we define a Hamiltonian of the Slater-Koster[16] type to describe d-band electrons on polytope 120. This model is relevant to transition-metal glasses. We diagonalize this Hamiltonian using the eigenfunctions found in part A, and obtain exact expressions

for the eigenvalues.

In Sec. III, we evaluate the eigenvalues using realistic values of coupling constants, and we discuss the resulting band structures. We find discrepancies between the polytope band structure and the crystalline band structure. Discrepancies arising from the differing short-range order interest us especially. The most striking discrepancies of this type are the gaps in the middle of the valence and conduction bands in polytope 240, and the absence of d-band splitting at the center of the Brillouin zone in polytope 120.

DiVincenzo et $al.$[9] have numerically diagonalized a realistic tight-binding model on polytope 240. They demonstrate the existence of an indirect band gap in their

model. We apply our d-band solution to understand trends in band ferromagnetism in amorphous transition metals.

I. STRUCTURE OF POLYTOPE 120

Coxeter[6] described how 120 atoms can pack in S^3 in such a way that each atom has icosahedral coordination. We construct fragments of this polytope in $\mathbb{R}^3$ (Fig. 1).

The sphere S^3 is isomorphic with the group SU(2). We give coordinates for atoms in polytope 120 in terms of corresponding SU(2) matrices. We recognize the resulting 120-element subspace of SU(2) as Y', the rotational symmetry group of an icosahedron. This fact immediately
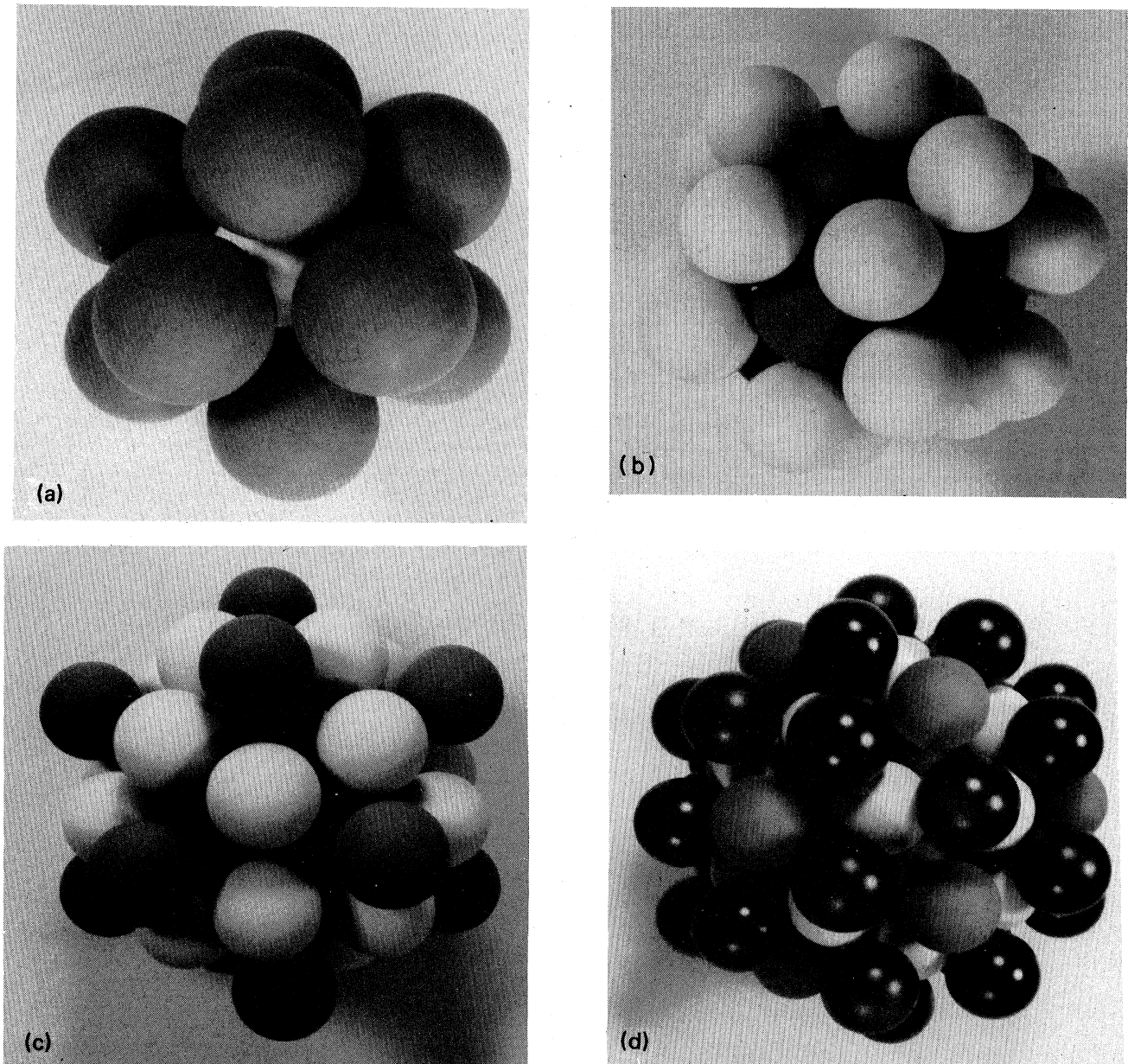

FIG. 1. Fragments of polytope 120 in R^3. (a) Coordination shell V_1 forms an icosahedron. (b) Coordination shell F_2 forms a dodecahedron. (c) Coordination shell V_3 forms an icosahedron. (d) Coordination shell E_4 forms an icosidodecahedron.

yields the following result: The rotational symmetry group G of polytope 120 is homomorphic to the direct square of Y'.

In this paper, we diagonalize explicitly several Hamiltonians defined on polytope 120. We accomplish this through analysis of the symmetry group G. Eigenfunctions of the Hamiltonians form the bases for irreducible representations of G, because these Hamiltonians commute with every element of G. The simple relationship between G and Y' allows us to express the representations of G as direct products of representations of Y'. We conclude Sec. I with a summary of the theory of representations of G.

We construct a fragment of polytope 120 in $\mathbb{R}^3$ by packing atoms around one central atom. We assign each coordination shell a name which describes the location of atoms with respect to an icosahedron centered on the central atom. Each new coordination shell is arranged to give atoms in previous coordination shells approximate icosahedral coordination.

Starting with the central atom C_0, we place 12 atoms in the first coordination shell V_1. These atoms sit at the vertices of an icosahedron [Fig. 1(a)]. The icosahedral coordination of C_0 is complete.

We place the second and third coordination shells of C_0 in such a way that atoms in V_1 have icosahedral coordination. We accomplish this by placing 20 atoms in the second coordination shell F_2, and placing 12 atoms in the third coordination shell V_3. Atoms in F_2 sit on the faces of V_1 [Fig. 1(b)]. Atoms in V_3 sit above the vertices of V_1 [Fig. 1(c)]. The icosahedral coordination of V_1 is now complete.

Finally, we complete the icosahedral coordination of F_2 by placing 30 atoms in the fourth coordination shell E_4. These atoms sit above the edges of V_1 [Fig. 1(d)]. We have now formed a 75-atom cluster in $\mathbb{R}^3$ in which 33 atoms have icosahedral coordination. We cannot extend this cluster without introducing defects, because of the frustration[3,17] of tiling $\mathbb{R}^3$ with icosahedra.

Frustration appears in our atomic clusters through the gaps between surface atoms. The edge length of an icosahedron is $1.05146\ldots$ times as large as the center-to-vertex distance. This creates gaps between atoms in V_1 which are 5% of an atomic diameter. With each successive coordination shell the gaps grow larger (Fig. 1).

The gaps in the fourth shell E_4 are large enough that two atoms could be placed on each edge instead of just one (atoms are "soft spheres"). The 105-atom cluster which results from this construction occurs in the Frank-Kasper phase of $Mg_{32}(Al,Zn)_{49}$. Each aluminum and zinc atom in this crystal has icosahedral coordination.[18]

Because of the frustration, additional coordination shells are unlikely to be physically significant. We introduce a set of coordinates for S^3 which help us describe polytope 120. Every point on S^3 defines a unit 4-vector,

$$u = (w,x,y,z) \in S^3 . \tag{1.1}$$

We can also write an arbitrary $u \in S^3$ as

$$u = (\cos\psi, \hat{n}\sin\psi) , \tag{1.2}$$

where ψ is the geodesic distance between u and the north pole $(1,0,0,0)$, and $\hat{n} \in S^2$ is a unit 3-vector. An isomorphism[19] exists between the sphere S^3 and the group SU(2),

$$(w,x,y,z) \in S^3 \leftrightarrow \begin{pmatrix} w+iz & ix+y \\ ix-y & w-iz \end{pmatrix} \in SU(2) . \tag{1.3}$$

Using the coordinates of Eq. (1.2), we write

$$u = e^{i\psi\hat{n}\cdot\sigma} \in SU(2) , \tag{1.4}$$

where σ is the vector of Pauli matrices.

We interpret each point $u \in S^3$ as a rotation of S^2 by the angle 2ψ around the axis $\hat{n}$. This interpretation follows from the isomorphism (1.3) between S^3 and SU(2), and the homomorphism[19] between SU(2) and SO(3). Thus each atom of polytope 120 corresponds to a rotation of S^2. We now list the coordination shells of polytope 120.

Begin with the central atom placed at the north pole

$$C_0 = \{u = 1\} . \tag{1.5a}$$

The first coordination shell has 12 members,

$$V_1 = \{u = e^{i(\pi/5)\hat{n}\cdot\sigma}: \hat{n} \text{ points to vertices of an icosahedron}\} . \tag{1.5b}$$

The second coordination shell has 20 members,

$$F_2 = \{u = e^{i(\pi/3)\hat{n}\cdot\sigma}: \hat{n} \text{ points to faces of an icosahedron}\} . \tag{1.5c}$$

The third coordination shell has 12 members,

$$V_3 = \{u^2: u \in V_1\} . \tag{1.5d}$$

The fourth coordination shell has 30 members,

$$E_4 = \{u = e^{i(\pi/2)\hat{n}\cdot\sigma}: \hat{n} \text{ points to edges of an icosahedron}\} . \tag{1.5e}$$

The fifth coordination shell has 12 members,

$$V_5 = \{ -u^2 : u \in V_1 \} .$$ (1.5f)

The sixth coordination shell has 20 members,

$$F_6 = \{ -u : u \in F_2 \} .$$ (1.5g)

The seventh coordination shell has 12 members,

$$V_7 = \{ -u : u \in V_1 \} .$$ (1.5h)

Finally, the eighth coordination shell has only one member,

$$C_8 = \{ u = -1 \} .$$ (1.5i)

Consider the rotations of S^2 induced by the SU(2) matrices in Eq. (1.5). The sets C_0 and C_8 correspond to the identity in SO(3). The sets V_1 and V_7 correspond to rotations by $2\pi/5$ around axes pointing through the vertices of an icosahedron inscribed in S^2. The sets F_2 and F_6 correspond to rotations by $2\pi/3$ around axes pointing through the midpoint of the faces of the icosahedron. The sets V_3 and V_5 correspond to rotations by $4\pi/5$ around axes pointing through the vertices of the icosahedron. The set E_4 corresponds to rotations by π around axes pointing through the midpoints of the edges of the icosahedron.

We recognize that the SU(2) matrices in Eq. (1.5) comprise the group of rotations which leave the icosahedron inscribed in S^2 invariant. Thus polytope 120 is identical to the icosahedral double group $Y' \subset SU(2)$. Each coordination shell comprises one conjugacy class of Y'.

We now summarize the irreducible representations of the group Y'. We also exploit the homomorphism between SO(4) and SU(2)×SU(2) in order to compute G, the symmetry group of polytope 120. We conclude Sec. I by summarizing the irreducible representations of G.

Irreducible representations of SU(2) contain irreducible representations of Y' because Y' is a subgroup of SU(2). Spherical harmonics $Y_{M,m}(\theta,\phi)$ form a basis for the irreducible representation of SU(2), of dimension $d_M = 2M+1$, when M is an integer or half integer. The character of $u \in SU(2)$ in the representation M is

$$\chi_M^{SU(2)}(e^{i\psi\hat{n}\cdot\sigma}) = \sin[(2M+1)\psi]/\sin\psi .$$ (1.6)

We display the character table of the group Y' in Table I.

In Table I, we label irreducible representations of Y' according to the convention used by Nelson and Widom.[10]

We denote arbitrary irreducible representations of Y' by the lower-case Greek letters α, β, γ, and δ. Table I gives the dimension d_α of the representation α by $\chi_\alpha^{Y'}(C_0)$. We determine the number of times the representation M contains the irreducible representation α through the formula

$$N_{M\alpha}^{Y'} = \frac{1}{o(Y')} \sum_{u \in Y'} \left[\chi_M^{SU(2)}(u) \right]^* \chi_\alpha^{Y'}(u) .$$ (1.7)

When M contains α, we write the basis functions for α as

$$\psi_{M\alpha,m}(\theta,\phi) = \sum_\mu Q_{M\alpha,m}^\mu Y_{M,\mu}(\theta,\phi) .$$ (1.8)

The coefficients Q have been discussed extensively.[20-22] Raynal[21] showed how to obtain Q simply for any value of M. Damhus et al.[22] introduced a coordinate system in which all Q are real. We adopt this convention. The coefficients Q obey the following orthonormality conditions

$$\sum_{\alpha,m} Q_{M\alpha,m}^\mu Q_{M\alpha,m}^\nu = \delta_{\mu\nu} ,$$ (1.9a)

$$\sum_\mu Q_{M\alpha,m}^\mu Q_{M\beta,n}^\mu = \delta_{\alpha\beta}\delta_{mn} .$$ (1.9b)

We use the expression (1.8) to derive the representation matrices and coupling coefficients for the group Y'. Spherical harmonics transform under the group SU(2) through multiplication by the Wigner D matrix[23]

$$u : Y_{M,m}(\theta,\phi) \rightarrow D_{m'm}^M(u) Y_{M,m'}(\theta,\phi) .$$ (1.10)

Thus the irreducible representation α transforms under the group Y' through multiplication by the matrix

$$D_{m',m}^\alpha(u) = Q_{M\alpha,m}^\mu D_{\mu'\mu}^M(u) Q_{M\alpha,m'}^{\mu'} ,$$ (1.11)

where M is any spherical harmonic containing α.

Wigner D matrices have the Clebsch-Gordon series[23]

$$D_{l'l}^L(u) D_{m'm}^M(u)$$

$$= \sum_{N,n',n} \langle Ll'Mm' | Nn' \rangle_{SU(2)} D_{n'n}^N(u) \langle LlMm | Nn \rangle_{SU(2)} ,$$ (1.12)

where $\langle \ | \ \rangle_{SU(2)}$ denotes the coupling coefficients of the group SU(2). Inspecting Eq. (1.11), we derive the Clebsch-Gordon series for the group Y',

TABLE I. Character of table of icosahedral double group. $\Omega = (\sqrt{5}+1)/2$ is the golden mean.

Y'	$1C_0$	$12V_1$	$20F_2$	$12V_3$	$30E_4$	$12V_5$	$20F_6$	$12V_1$	$1C_8$
A	1	1	1	1	1	1	1	1	1
E_1	2	Ω	1	Ω^{-1}	0	$-\Omega^{-1}$	-1	$-\Omega$	-2
E_2	2	$-\Omega^{-1}$	1	$-\Omega$	0	Ω	-1	Ω^{-1}	-2
F_1	3	Ω	0	$-\Omega^{-1}$	-1	$-\Omega^{-1}$	0	Ω	3
F_2	3	$-\Omega^{-1}$	0	Ω	-1	Ω	0	$-\Omega^{-1}$	3
G_1	4	1	-1	-1	0	1	1	-1	-4
G_2	4	-1	1	-1	0	-1	1	-1	4
H	5	0	-1	0	1	0	-1	0	5
I	6	-1	0	1	0	-1	0	1	-6

$$D_{l'l}^{\alpha}(u)D_{m'm}^{\beta}(u)$$
$$= \sum_{\gamma,n',n,r} \langle \alpha l'\beta m' \mid \gamma n'r \rangle_{Y'} D_{n'n}^{\gamma}(u)\langle \alpha l\beta m \mid \gamma nr \rangle_{Y'} .$$

$$(1.13)$$

The icosahedral coupling coefficient is defined by

$$\langle L\alpha M\beta \mid\mid N\gamma r \rangle_{Y'}\langle \alpha l\beta m \mid \gamma nr \rangle_{Y'}$$
$$= \sum_{\lambda,\mu,\nu} Q_{L\alpha,l}^{\lambda}Q_{M\beta,m}^{\mu}Q_{N\gamma,n}^{\nu}\langle L\lambda M\mu \mid N\nu \rangle_{\mathrm{SU}(2)} . \quad (1.14)$$

In Eq. (1.14), we choose L, M, and N to be the lowest spherical harmonics containing, respectively, α, β, and γ. If the product of α and β contains γ more than once, then we must take additional values of L, M, or N. The multiplicity index r distinguishes between occurrences of γ in the product of α and β. We usually suppress the index r in complicated expressions. Pooler[20] gives a complete table of coupling coefficients for the group $Y \subset \mathrm{SO}(2)$. Damhus et al.[22] discuss the appropriate assignment of L, M, and N values for different r.

The isoscalar symbol $\langle \mid\mid \rangle_{Y'}$ in Eq. (1.14) is chosen so that the icosahedral coupling coefficients obey the orthonormality relations

$$\sum_{l,m} \langle \alpha l\beta m \mid \gamma'n'r' \rangle\langle \alpha l\beta m \mid \gamma nr \rangle = \delta_{\gamma'\gamma}\delta_{n'n}\delta_{r'r} , \quad (1.15a)$$

and

$$\sum_{\gamma,n,r} \langle \alpha l'\beta m' \mid \gamma nr \rangle\langle \alpha l\beta m \mid \gamma nr \rangle = \delta_{l'l}\delta_{m'm} . \quad (1.15b)$$

We generalize the preceding results to $G \subset \mathrm{SO}(4)$, the symmetry group of polytope 120. First, we note a simple relationship between G and Y'. Consider $l,r \in Y'$, and transform Y' by

$$(l,r): \quad Y' \to lY'r^{-1} . \quad (1.16)$$

Because Y' is a group,

$$lY'r^{-1} = Y' , \quad (1.17)$$

so the transformation (1.16) is a symmetry of polytope 120. The angle[10] between $u,v \in S^3$,

$$\psi(u,v) = \cos^{-1}(\tfrac{1}{2}\mathrm{Tr}uv^{-1}) , \quad (1.18)$$

is preserved under (1.16). Thus the transformation (1.16) is orthogonal. Finally, noting that $(-l,-r)$ induces the same transformation as (l,r), we obtain

$$G = Y' \otimes Y'/Z_2 . \quad (1.19)$$

We use the relation (1.19) to relate irreducible representations of G to irreducible representations of Y'. First, consider the analogous problem of relating SO(4) and SU(2). We have, in analogy with (1.19),

$$\mathrm{SO}(4) = \mathrm{SU}(2) \otimes \mathrm{SU}(2)/Z_2 . \quad (1.20)$$

Diagonal[10] irreducible representations of SO(4) are generated by the hyperspherical harmonics $Y_{M,m_1m_2}(u)$. Hyperspherical harmonics are related[24] to the Wigner D matrices by

$$Y_{M,m_1m_2}(u) = \left[\frac{M+1}{2\pi^2}\right]^{1/2} D_{m_1m_2}^{M/2}(u) . \quad (1.21)$$

The hyperspherical harmonic transforms as

$$(l,r): \quad Y_{M,m_1m_2}(u) \to D_{m_1m_1'}^{M/2}(l)Y_{M,m_1'm_2'}(u)D_{m_2'm_2}^{M/2}(r^{-1}) . \quad (1.22)$$

Thus we find the representation matrices of SO(4) are the direct product of representation matrices of SU(2). The characters of SO(4) factor into characters of SU(2)

$$\chi_M^{\mathrm{SO}(4)}(l,r) = \chi_{M/2}^{\mathrm{SU}(2)}(l)\chi_{M/2}^{\mathrm{SU}(2)}(r^{-1}) . \quad (1.23)$$

Hyperspherical harmonics contain irreducible representations of G. We label representations with a pair of Greek letters. We write

$$\psi_{M\alpha\beta,m_1m_2}(u) = \sum_{\mu_1\mu_2} Q_{M\alpha\beta,m_1m_2}^{\mu_1\mu_2}Y_{M,\mu_1\mu_2}(u) , \quad (1.24)$$

where the Q coefficients of the group G factor[12] into products of Q coefficients of the group Y',

$$Q_{M\alpha\beta,m_1m_2}^{\mu_1\mu_2} = Q_{M\alpha,m_1}^{\mu_1}Q_{M\beta,m_2}^{\mu_2} . \quad (1.25)$$

It follows that basis functions transform as

$$(l,r): \quad \psi_{M\alpha\beta,m_1m_2}(u) \to D_{m_1m_1'}^{\alpha}(l)\psi_{M\alpha\beta,m_1'm_2'}(u)D_{m_2'm_2}^{\beta}(r^{-1}) . \quad (1.26)$$

Characters of G factor into characters of Y'

$$\chi_{\alpha\beta}^G(l,r) = \chi_{\alpha}^{Y'}(l)\chi_{\beta}^{Y'}(r^{-1}) . \quad (1.27)$$

In Sec. II, we show that the basis functions of irreducible representations of G are eigenfunctions of simple Hamiltonians defined on polytope 120. The results (1.24)–(1.27) allow explicit calculations of energy spectra.

II. TIGHT-BINDING MODELS

A. Polytope 120, s orbitals

The simplest tight-binding model describes electrons hopping between s orbitals of neighboring atoms. The hopping matrix element has no angular dependence in this case. The Hamiltonian takes the simple form[10]

$$H^s = V \sum_{u \in Y'} \sum_{v \in V_1} \mid u \rangle\langle vu \mid . \quad (2.1)$$

The hopping matrix element V is typically negative and we normalize it to

$$V = -1 . \quad (2.2)$$

Eigenfunctions of H fall into groups, with degeneracy d_α^2, which form bases for irreducible representations $\alpha\alpha$ of G:

$$\mid M\alpha m_1m_2 \rangle = \sum_{u \in Y'} \psi_{M\alpha\alpha,m_1m_2}(u) \mid u \rangle , \quad (2.3)$$

where the basis function ψ is defined by Eq. (1.24). Matrix elements of the Hamiltonian are

$$\langle M\alpha m_1 m_2 \,|\, H^s \,|\, N\beta n_1 n_2 \rangle$$
$$= \sum_{u\in Y'} \sum_{v\in V_1} \psi^*_{M\alpha\alpha,m_1 m_2}(u)\psi_{N\beta\beta,n_1 n_2}(vu) \ . \quad (2.4)$$

Using the transformation property of the basis function (1.26) we find

$$\langle M\alpha m_1 m_2 \,|\, H^s \,|\, N\beta n_1 n_2 \rangle = -\delta_{\alpha\beta}\delta_{m_2 n_2} \sum_{v\in V_1} D^{\beta}_{n_1 m_1}(v) \ .$$
$$(2.5)$$

Note that V_1, the set of nearest neighbors of the north pole in Y', is a conjugacy class of Y'. This means that the sum in (2.5) commutes with $D^{\beta}(u)$ for all $u \in Y'$. Schur's lemma yields the result

$$\sum_{v\in V_1} D^{\beta}_{n_1 m_1}(v) = \delta_{n_1 m_1} o(V_1)\chi^{Y'}_{\beta}(V_1)/d_{\beta} \ . \quad (2.6)$$

We find the spectrum of H^s is

$$E^s_{\alpha} = -o(V_1)\chi^{Y'}_{\beta}(V_1)/d_{\beta} \quad (2.7)$$

with degeneracy

$$D^s_{\alpha} = d^2_{\alpha} \ . \quad (2.8)$$

Equations (2.7) and (2.8) agree with numerical results of Warner[25] and semianalytical results of Mosseri and Sadoc.[26]

The results of Mosseri and Sadoc suggest the existence of a polytope reciprocal space. They find an axis of $\{30/11\}$ screw symmetry and then partially diagonalize H^s using the corresponding 30-element Abelian subgroup of G. Each eigenfunction of H^s has a wave number $k = 2\pi n/30$ ($n = 0,1,2,\ldots,29$) along this axis. For each wave number k, there are $\frac{120}{30} = 4$ associated eigenfunctions.

We wish to find additional quantum numbers which will uniquely identify eigenfunctions of H^s. Crystals in $\mathbb{R}^3$ have two additional quantum numbers which are wave numbers in the two additional orthogonal directions. The three crystal wave numbers define a wave vector $\mathbf{k}$ for each eigenfunction. It appears impossible to define a wave vector, in the conventional sense, on the polytope because of the curvature of S^3. Reciprocal lattice vectors, for example, have a matrix character.[10]

We associate a wave number[10] $k = \sqrt{M(M+2)}$ with each degenerate block of eigenfunctions contained in the hyperspherical harmonic M. The two additional independent quantum numbers that uniquely identify eigenfunctions are m_1 and m_2. However, we cannot identify m_1 and m_2 as wave numbers along independent directions in the polytope. Thus we cannot define the angular components of the wave vector $\mathbf{k}$.

X-ray scattering probes the structure of reciprocal space experimentally. Powder diffraction experiments average over the angular part of the wave vector $\mathbf{k}$. Thus we identify the wave number

$$k = \sqrt{M(M+2)} \approx M \quad (2.9)$$

as a physically relevant quantity.[10,11] When the hyperspherical harmonic M contains the unit representation of

Y', Bragg peaks occur in the x-ray structure function. These values of M belong to the set[10]

$$\mathscr{B} = \{0,12,20,24,30,32,\ldots\} \ . \quad (2.10)$$

We expect large deviations of the spectrum (2.7) and (2.8) from the free electron spectrum,

$$E^f_M = M(M+2)-12, \quad D^f_M = (M+1)^2 \ , \quad (2.11)$$

when the wave number is one-half the wave number corresponding to a Bragg peak. Such perturbations signal the existence of Brillouin zones for polytope 120. These perturbations appear in the splitting of energy levels (2.11) when $2M \in \mathscr{B}$.

Figure 2 shows the energies of eigenfunctions of H^s contained in the hyperspherical harmonic M. Thus we have an angular averaged, repeated zone spectrum. The $\pm$ signs on the M axis identify values for which $2M \in \mathscr{B}$. We use a $+$ sign when M is even and a $-$ sign when M is odd. The first splitting[21] of (2.11) occurs when $M = 6$. Remarkably, 2×6 is the first nonzero element of $\mathscr{B}$. The second splitting occurs when $M = 10$. Note that 2×10 is the second nonzero element of $\mathscr{B}$.

We find that the number of irreducible representations of Y', contained in the hyperspherical harmonic Y_M, increases by one whenever M is even and $2M \in \mathscr{B}$. This number decreases by one whenever M is odd and $2M \in \mathscr{B}$. (This is not clear in Fig. 2 because often Y_M contains the same irreducible representation more than once.) Even more striking is the minimum of the disperson curve at every Bragg peak. This coincidence of x-ray scattering and electronic structure strongly suggests that some analog of Brillouin zones exists for polytope 120.

B. Polytope 240, sp^3 hybrid orbitals

Weaire and Thorpe[13] define a simple tight-binding model for tetracoordinated semiconductors. Although they base their model on sp^3 hybrid orbitals, a simple transformation[14] reduces it to an s orbital model on the same network. When the network contains only even numbered rings, we can subdivide it into two interpenetrating sublattices. Polytope 240 is such a network.
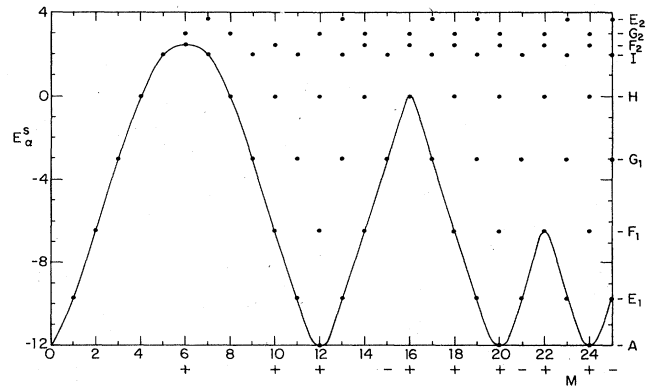

FIG. 2. Repeated zone spectrum of H^s. Energy levels are labeled by irreducible representations of Y'. Even (odd) values of M for which $2M \in \mathscr{B}$ are labeled with a $+$ ($-$) sign.

We relate the energy spectrum on the full network to the spectra of its sublattices.

We construct polytope 240 as follows. Sublattice A of polytope 240 consists of polytope 120. Sublattice B of polytope 240 consists of the points $\tau Y'$ where $\tau \in S^3$ denotes the center of one of the 20 tetrahedral cells surrounding the north pole in polytope 120. If we multiply Y' on the right by τ instead of on the left, we create polytope 240 with the opposite chirality. Chirality does not affect the band structure.

One atom of sublattice A of polytope 240 lies at the north pole. This atom has four neighbors which belong to sublattice B and will be denoted $\{\sigma_i: i=1, \ldots, 4\}$. Clearly, τ is a member of this set. Any point $u \in A$ has neighbors $\{\sigma_i u\} \subset B$. Any point $u \in B$ has neighbors $\{\sigma_i^{-1} u\} \subset A$.

We define four orbital states[13] on each site $\{|u,\sigma_i\rangle\}$, where u is a site of polytope 240 and σ_i defines the near neighbors of u. Straley[15] defines the operators

$$\hat{U} = \frac{1}{4} \sum_{u \in Y'} \sum_{i,j} |u,\sigma_i\rangle\langle u,\sigma_j| \ , \tag{2.12}$$

and

$$\hat{T} = \sum_i \left[\sum_{u \in A} |u,\sigma_i\rangle\langle \sigma_i u,\sigma_i| + \sum_{u \in B} |u,\sigma_i\rangle\langle \sigma_i^{-1} u,\sigma_i| \right] \cdot \tag{2.13}$$

The Weaire and Thorpe Hamiltonian is

$$H^{sp^3} = 4V_1 \hat{U} + V_2 \hat{T} - V_1 \ . \tag{2.14}$$

Eigenvalues of H^{sp^3} are given by

$$E^{sp^3} = V_1 \pm (4V_1^2 + V_1 V_2 \epsilon + V_2^2)^{1/2} \ , \tag{2.15}$$

where ϵ is an eigenvalue of

$$H' = 4\hat{U}\hat{T}\hat{U} \ . \tag{2.16}$$

In addition, there are N localized states with energy $-V_1 - V_2$ and N localized states with energy $-V_1 + V_2$. The number of atoms N is 240.

Consider the new Hamiltonian H' (2.16). Using the explicit forms (2.12) and (2.13) of $\hat{U}$ and $\hat{T}$, we rewrite (2.16) as

$$H' = \sum_i \left[\sum_{u \in A} |u\rangle\langle \sigma_i u| + \sum_{\omega \in B} |\omega\rangle\langle \sigma_i^{-1}\omega| \right] , \tag{2.17}$$

where $|u\rangle$ denotes an electron sitting at site u. H' is thus an s-orbital Hamiltonian for polytope 240. We now relate H' to H^s, the s orbital Hamiltonian on polytope 120.

Just as a diamond lattice can be considered an fcc lattice with two atoms per unit cell, we can consider polytope 240 as polytope 120 with two atoms per unit cell. Associated with each atom $u \in A$ there is an atom $\tau u \in B$. We use this fact to construct eigenfunctions for H' based on the eigenfunctions for H^s that we derived in part A of this section.

Assume that the polytope 240 wave functions on sublattice A are proportional to eigenfunctions of H^s. Define

$$\phi_\alpha^A = \sum_{u \in A} \psi_\alpha(u) |u\rangle \ , \tag{2.18}$$

where ψ_α denotes one of the irreducible basis functions (1.24). ϕ_α^A lies in the null space of the first term of Eq. (2.17). The second term in (2.17) sums ϕ_α^A over the vertices of tetrahedral cells and places the resulting amplitude at the center of the cell. Thus

$$H'\phi_\alpha^A = \sum_{\omega \in B} \sum_i \psi_\alpha(\sigma_i^{-1}\omega) |\omega\rangle \ . \tag{2.19}$$

The polytope 240 wave function contains ϕ_α^A only if it contains $H'\phi_\alpha^A$. Thus we define

$$\phi_\alpha^B = H'\phi_\alpha^A \ . \tag{2.20}$$

Consider the action of H' on ϕ_α^B. ϕ_α^B lies in the null space of the second term in Eq. (2.17). We find

$$H'\phi_\alpha^B = \sum_{u \in A} \sum_{i,j} \psi_\alpha(\sigma_i^{-1}\sigma_j u) |u\rangle \ . \tag{2.21}$$

Examine the set

$$S = \{\sigma_i^{-1}\sigma_j\} \subset A \ , \tag{2.22}$$

which occurs in the sum in Eq. (2.21). When $i=j$, $\sigma_i^{-1}\sigma_j = 1$, so S contains the north pole four times. In general, we note that $\sigma_i^{-1}\sigma_j$ are the vertices of tetrahedral cells of polytope 120 containing σ_j. When $i \neq j$, $\sigma_i^{-1}\sigma_j$ are the twelve vertices of the icosahedron surrounding the north pole. Thus

$$S = \{1,1,1,1,V_1\} \ . \tag{2.23}$$

We find

$$H'\phi_\alpha^B = \sum_{u \in A} \left[4\psi_\alpha(u) + \sum_{v \in V_1} \psi_\alpha(vu) \right] |u\rangle \ . \tag{2.24}$$

Note that the second term in Eq. (2.24) is just $-H^s$ acting on ψ_α. Thus, H' becomes a 2×2 matrix in the basis of ϕ_α^A and ϕ_α^B,

$$H' = \begin{bmatrix} 0 & 1 \\ 4-H^s & 0 \end{bmatrix} \cdot \tag{2.25}$$

Eigenvalues of H' are

$$\epsilon_\alpha' = \pm(4 - E_\alpha^s)^{1/2} \ . \tag{2.26}$$

Equation (2.15) yields the sp^3 hybrid density of states from our result (2.26). We now have an exact solution to the sp^3 band structure of polytope 240. Next we solve the d-band structure of polytope 120.

C. Polytope 120 d orbitals

Transition-metal d bands are frequently analyzed with tight-binding models.[27] Slater and Koster[16] introduce a particularly simple model based on the two-center approximation. We will adapt the model of Slater and Koster to polytope 120 and diagonalize it analytically.

Electrons in d orbitals in $\mathbb{R}^3$ have atomic wave functions

$$\Psi_a(\mathbf{r}) = Y_{2,a}(\mathbf{r}) f(|\mathbf{r}|) \tag{2.27}$$

where the spherical harmonic depends only on the angular part of $\mathbf{r} \in R^3$. The tight-binding overlap integrals form a matrix,

$$V_{ab}(\hat{n}) = \int d^3\mathbf{r} \Psi_a^*(\mathbf{r}-\hat{n})\Delta(\mathbf{r})\Psi_b(\mathbf{r}) , \qquad (2.28)$$

where $\hat{n} \in S^2$ points from atom b to atom a. We assume atomic spacing is equal to one. The potential energy $\Delta(\mathbf{r})$ has the point-group symmetry of the site of atom b.

We adapt Eq. (2.28) to polytope 120 by defining the overlap integral in S^3 as the integral (2.28) in $\mathbb{R}^3$ where $\hat{n}$ defines the direction of v (1.2). Thus

$$V_{ab}(v) = V_{ab}(\hat{n}) , \qquad (2.29)$$

where $v \in V_1$. With this definition, $V_{ab}(v)$ has the correct transformation properties.

It is instructive to study the dependence of V_{ab} on $\hat{n}$. Consider first

$$\omega = (\cos\pi/5, \hat{z}\sin\pi/5) \in V_1 . \qquad (2.30)$$

Symmetries of the spherical harmonics reveal

$$V_{ab}(\omega) = \begin{vmatrix} \delta & 0 & 0 & 0 & 0 \\ 0 & \pi & 0 & 0 & 0 \\ 0 & 0 & \sigma & 0 & 0 \\ 0 & 0 & 0 & \pi & 0 \\ 0 & 0 & 0 & 0 & \delta \end{vmatrix} , \qquad (2.31)$$

where the independent overlap integrals σ, π, and δ are phenomenological parameters. Any other $v \in V_1$ has the form $v = u\omega u^{-1}$. Let R_u be the operator which rotates $\hat{n}$ under the homomorphism SU(2)$\rightarrow$SO(3). Equation (2.28) yields

$$V_{ab}(u\omega u^{-1}) = \int_{\mathbb{R}^3} d^3\mathbf{r} \Psi_a^*(\mathbf{r}-R_u\hat{n})\Delta(\mathbf{r})\Psi_b(\mathbf{r}) \qquad (2.32)$$

$$= \int_{\mathbb{R}^3} d^3\mathbf{r} \Psi_a^*(R_u(\mathbf{r}-\hat{n}))\Delta(\mathbf{r})\Psi_b(R_u\mathbf{r}) . \qquad (2.33)$$

We used the symmetry of Δ to derive Eq. (2.33).

Atomic wave functions Ψ_a form a basis for the five dimensional representation H of Y'. Thus

$$\Psi_a(R_u\mathbf{r}) = D_{a'a}^H(u)\Psi_{a'}(\mathbf{r}) , \qquad (2.34)$$

and therefore

$$V_{ab}(u\omega u^{-1}) = [D_{a'a}^H(u)]^* V_{a'b'}(\omega)D_{b'b}^H(u) . \qquad (2.35)$$

Unitarity of the D matrices, and reality of $V_{ab}(\omega)$, reveal

$$V_{ab}(uvu^{-1}) = D_{aa'}^H(u)V_{ab}(\omega)D_{b'b}^H(u^{-1}) . \qquad (2.36)$$

Thus $V_{ab}(v)$ transforms like the irreducible representation matrix D^H, within the class $V_1 \subset Y'$. $V_{ab}(v)$ is undefined outside the class V_1.

Our Hamiltonian,

$$H^d = \sum_{u \in Y'} \sum_{v \in V_1} \sum_{a,b} |u,a\rangle V_{ab}(v)\langle vu,b| , \qquad (2.37)$$

describes atoms hopping from orbital b at site vu to orbital a at the neighboring site u. We expand eigenfunctions of H^d in terms of eigenfunctions of H^s. Define

$$|M\alpha m_1 m_2 a\rangle = \sum_{u \in Y'} \Psi_{M\alpha\alpha,m_1 m_2}(u) |u,a\rangle . \qquad (2.38)$$

Matrix elements of the Hamiltonian are

$$\langle M\alpha m_1 m_2 a | H^d | N\beta n_1 n_2 b\rangle$$
$$= \sum_{u \in Y'} \sum_{v \in V_1} \sum_{a,b} \psi_{M\alpha\alpha,m_1 m_2}^*(u)V_{ab}(v)\psi_{N\beta\beta,n_1 n_2}(vu) , \qquad (2.39)$$

which is equivalent to Eq. (2.4) with a direction-dependent hopping matrix. Following the development of part A, we find

$$\langle M\alpha m_1 m_2 a | H^d | N\beta n_1 n_2 b\rangle$$
$$= \delta_{\alpha\beta}\delta_{m_2 n_2} \sum_{v \in V_1} V_{ab}(v)D_{n_1 m_1}^\beta(v) . \qquad (2.40)$$

We cannot apply Schur's lemma to Eq. (2.40) because the product of D^β with V_{ab} is not, in general, an irreducible representation matrix. We can still diagonalize the Hamiltonian H^d.

First, we perform much algebra. Using the conjugacy invariance of the classes of Y', we write

$$\sum_{v \in V_1} V_{ab}(v)D_{n_1 m_1}^\beta(v)$$
$$= \frac{o(V_1)}{o(Y')} \sum_{u \in Y'} V_{ab}(u\omega u^{-1})D_{n_1 m_1}^\beta(u\omega u^{-1}) , \qquad (2.41)$$

where ω is the standard element of V_1 defined in Eq. (2.30). Now, we relate the matrices in Eq. (2.41) evaluated at $u\omega u^{-1}$, to the same matrices evaluated at ω. Equation (2.36) yields

$$\sum_{v \in v_1} V_{ab}(v)D_{n_1 m_1}^\beta(v) = \frac{o(V_1)}{o(Y')}\left[\sum_{u \in Y'} D_{aa'}^H(u)D_{b'b}^H(u^{-1})D_{n_1 n'}^\beta(u)D_{m'm_1}^\beta(u^{-1})\right]V_{a'b'}(\omega)D_{n'm'}^\beta(\omega) . \qquad (2.42)$$

We apply the Clebsh-Gordon series (1.13),

$$D_{aa'}^H(u)D_{n_1 n'}^\beta(u)D_{b'b}^H(u^{-1})D_{m'm_1}^\beta(u^{-1})$$
$$= \sum_{\gamma,c,c'} \sum_{\delta,d,d'} \langle Ha\beta n_1 | \gamma c\rangle_{Y'} D_{cc'}^\gamma(u)\langle Ha'\beta n' | \gamma c'\rangle_{Y'}\langle Hb'\beta m' | \delta d'\rangle_{Y'} D_{d'd}^\delta(u^{-1})\langle Hb\beta m_1 | \delta d\rangle_{Y'} . \qquad (2.43)$$

Noting that

$$\sum_{u \in Y'} D_{cc'}^\gamma(u)D_{d'd}^\delta(u^{-1}) = \delta_{\gamma\delta}\delta_{cd}\delta_{c'd'}o(Y')/d_\gamma , \qquad (2.44)$$

TABLE II. Energy spectrum of H^d. Letters in left-hand column label irreducible representations β and γ. The number is the degeneracy $D^d_{\beta\gamma}$. The right-hand column shows $E^d_{\beta\gamma}$ evaluated by Eq. (2.48).

5 AH	$\frac{12}{5}\sigma$	$+$	$\frac{24}{5}\pi$	$+$	$\frac{24}{5}\delta$
8 E_1G_1	$\frac{6\Omega}{5}\sigma$	$+$	$\frac{12\Omega}{5}\pi$	$+$	$\frac{12\Omega}{5}\delta$
12 E_1I	$\frac{6\Omega}{5}\sigma$	$+$	$\frac{12\Omega}{5}\pi$	$+$	$\frac{12\Omega}{5}\delta$
8 E_2G_1	$\frac{6}{5}(1-\Omega)\sigma$	$+$	$\frac{12}{5}(1-\Omega)\pi$	$+$	$\frac{12}{5}(1-\Omega)\delta$
12 E_2I	$\frac{6}{5}(1-\Omega)\sigma$	$+$	$\frac{12}{5}(1-\Omega)\pi$	$+$	$\frac{12}{5}(1-\Omega)\delta$
9 F_1F_1	$\frac{2\Omega+6}{5}\sigma$	$+$	$\frac{6}{5}(\Omega+1)\pi$	$+$	$\frac{12}{5}(\Omega-1)\delta$
9 F_1F_2	$\frac{12}{5}\sigma$	$+$	$\frac{12}{5}(\Omega-1)\pi$	$+$	$\frac{8\Omega}{5}\delta$
12 F_1G_2	$\frac{6}{5}(\Omega-1)\sigma$	$+$	$\frac{4}{5}(\Omega+3)\pi$	$+$	$\frac{2}{5}(5\Omega-3)\delta$
15 F_1H	$\frac{6}{5}(\Omega-1)\sigma$	$+$	$\frac{2}{5}(5\Omega-3)\pi$	$+$	$\frac{4}{5}(\Omega+3)\delta$
9 F_2F_1	$\frac{12}{5}\sigma$	$+$	$\frac{8}{5}(1-\Omega)\pi$	$-$	$\frac{12\Omega}{5}\delta$
9 F_2F_2	$\frac{2}{5}(4-\Omega)\sigma$	$-$	$\frac{12\Omega}{5}\pi$	$+$	$\frac{6}{5}(2-\Omega)\delta$
12 F_2F_2	$-\frac{6\Omega}{5}\sigma$	$+$	$\frac{2}{5}(2-5\Omega)\pi$	$+$	$\frac{4}{5}(4-\Omega)\delta$
15 F_2H	$-\frac{6\Omega}{5}\sigma$	$+$	$\frac{4}{5}(4-\Omega)\pi$	$+$	$\frac{2}{5}(2-5\Omega)\delta$
8 G_1E_1	$\frac{6\Omega}{5}\sigma$	$+$	$\frac{3}{5}(1+2\Omega)\pi$	$+$	$\frac{12}{5}(1-\Omega)\delta$
8 G_1E_2	$\frac{6}{5}(1-\Omega)\sigma$	$+$	$\frac{12\Omega}{5}\pi$	$+$	$\frac{3}{5}(3-2\Omega)\delta$
16 G_1G_1	$\frac{3}{5}\sigma$	$+$	$\frac{6}{5}\pi$	$+$	$\frac{6}{5}\delta$
24 G_1I	$\frac{6}{35}(6-5\Omega)\sigma$	$+$	$\frac{3}{35}(19-10\Omega)\pi$	$+$	$\frac{12}{35}(1+5\Omega)\delta$
24 $\widetilde{G}_1I$	$\frac{6}{35}(1+5\Omega)$	$+$	$\frac{12}{35}(4-\Omega)\pi$	$+$	$\frac{3}{35}(17-6\Omega)\delta$
12 G_2F_1	$\frac{6}{5}(\Omega-1)\sigma$	$+$	$\frac{4}{5}(\Omega-2)\pi$	$-$	$\frac{10\Omega+1}{5}\delta$
12 G_2F_2	$-\frac{6\Omega}{5}\sigma$	$+$	$\frac{10\Omega-11}{5}\pi$	$-$	$\frac{4}{5}(\Omega+1)\sigma$
16 G_2G_2	$-\frac{3}{5}\sigma$	$-$	$\frac{2}{5}(4\Omega+1)\pi$	$+$	$\frac{2}{5}(4\Omega+5)\delta$
20 G_2H	$-\frac{3}{5}\sigma$	$+$	$\frac{3}{10}(2\Omega-5)\pi$	$-$	$\frac{3}{10}(3+2\Omega)\delta$

TABLE II. (*Continued*).

20	$\widetilde{G}_2H$	$-\frac{3}{5}\sigma$	$-$	$\frac{1}{10}(7+10\Omega)\pi$	$+$	$\frac{10\Omega-17}{10}\delta$
5	HA	$\frac{12}{5}\sigma$	$+$	$\frac{12}{5}(\Omega-1)\pi$	$-$	$\frac{12\Omega}{5}\delta$
15	HF_1	$\frac{6}{5}(\Omega-1)\sigma$	$+$	$\frac{2}{5}(5-\Omega)\pi$	$-$	$\frac{4}{5}(\Omega+1)\delta$
15	HF_2	$-\frac{6\Omega}{5}\sigma$	$+$	$\frac{4}{5}(\Omega-2)\pi$	$+$	$\frac{2}{5}(4+\Omega)\delta$
20	HG_2	$-\frac{3}{5}\sigma$	$+$	$\frac{3}{5}(2-3\Omega)\pi$	$+$	$\frac{3}{5}(3\Omega-1)\delta$
20	$H\widetilde{G}_2$	$-\frac{3}{5}\sigma$	$+$	$\frac{7\Omega-2}{5}\pi$	$+$	$\frac{5-7\Omega}{5}\delta$
25	HH	$\frac{18}{35}(1-\Omega)\sigma$	$+$	$\frac{6}{35}(\Omega-5)\pi$	$+$	$\frac{12}{35}(1+\Omega)\delta$
25	$H\widetilde{H}$	$\frac{6}{35}(3\Omega+4)\sigma$	$+$	$\frac{4}{35}(4-5\Omega)\pi$	$+$	$\frac{2}{35}(\Omega-20)\delta$
12	IE_1	$\frac{6\Omega}{5}\sigma$	$+$	$\frac{4}{5}(2-\Omega)\pi$	$-$	$\frac{2}{5}(9+\Omega)\delta$
12	IE_2	$\frac{6}{5}(1-\Omega)\sigma$	$+$	$\frac{2}{5}(\Omega-10)\pi$	$+$	$\frac{4}{5}(\Omega+1)\delta$
24	IG_1	$\frac{6}{35}(6-5\Omega)\sigma$	$+$	$\frac{2}{35}(25\Omega-29)\pi$	$-$	$\frac{4}{35}(12+5\Omega)\delta$
24	$I\widetilde{G}_1$	$\frac{6}{35}(1+5\Omega)\sigma$	$+$	$\frac{4}{35}(5\Omega-17)\pi$	$-$	$\frac{2}{35}(4+25\Omega)\delta$
36	II	$\frac{15\Omega-49}{35}\sigma$	$-$	$\frac{6}{35}(3+5\Omega)\pi$	$+$	$\frac{3}{35}(5\Omega-1)\delta$
36	$I\widetilde{I}$	$-\frac{2}{105}(91+5\Omega)\sigma$	$-$	$\frac{2}{315}(164+19\Omega)\pi$	$+$	$\frac{4}{315}(61+17\Omega)\delta$
36	$I\widetilde{\widetilde{I}}$	$-\frac{1}{15}(1+5\Omega)\sigma$	$+$	$\frac{2}{45}(17-5\Omega)\pi$	$+$	$\frac{25\Omega-121}{45}\delta$

we combine Eqs. (2.42) and (2.43) to get

$$\sum_{v\in V_1} V_{ab}(v)D^{\beta}_{n_1m_1}(v)$$

$$=o(V_1)\left[\sum_{\gamma,c,c'}\langle Ha\beta n_1\,|\,\gamma c\rangle_{Y'}\langle Hb\beta m\,|\,\gamma c\rangle_{Y'}\langle Ha'\beta n'\,|\,\gamma c'\rangle_{Y'}\langle Hb'\beta m'\,|\,\gamma c'\rangle_{Y'}\right]V_{a'b'}(\omega)D_{n'm'}(\omega)\ .\quad(2.45)$$

We use Eq. (2.45) to diagonalize H^d. Multiply (2.45) by

$$\langle Ha\beta n_1\,|\,\delta d\rangle_{Y'}\langle Hb\beta m_1\,|\,\epsilon e\rangle_{Y'}\qquad(2.46)$$

and sum over a, b, m_1, and n_1. Orthonormality of the coupling coefficients (1.15) yields the result

$$\delta_{\delta\epsilon}\delta_{de}\frac{o(V_1)}{d\gamma}\langle Ha'\beta n'\,|\,\delta d\rangle_{Y'}\langle Hb'\beta m'\,|\,\epsilon e\rangle_{Y'}V_{a'b'}(\omega)D^{\beta}_{n'm'}(\omega)\ .\qquad(2.47)$$

Because $V(\omega)$ and $D^\beta(\omega)$ are diagonal, the spectrum of H^d is

$$E_{\beta\gamma}^d = \frac{o(V_1)}{d\gamma} \sum_{a,m,c} \langle Ha\beta m \mid \gamma c \rangle_{Y'}^2, V_{aa}(\omega)D_{mm}^\beta(\omega) \quad (2.48)$$

with degeneracy

$$D_{\beta\gamma}^d = d_\beta d_\gamma , \quad (2.49)$$

where β runs through all nine irreducible representations of Y', and γ runs through all irreducible representations of Y' in the Clebsch-Gordon series of $H\beta$. We evaluate Eq. (2.48) in Table II.

III. DENSITIES OF STATES

In Sec. II, we exactly solved three tight-binding models defined on polytopes. Only finite numbers of energy levels occur because of the finiteness of the polytopes. Strictly speaking, we can only present histograms of the energy spectra, not densities of states. However, we can smooth out the histograms to obtain a continuous curve. We interpret this smooth curve as the density of states of an amorphous material with short-range icosahedral order.

We refer to histograms of the energy spectra as densities of states. Figure 3(a) shows the density of states of H^s, the s band Hamiltonian on polytope 120. Compare Fig. 3(a) with Fig. 3(b) which shows the s band density of states of an fcc crystal[28] and a metallic glass.[29] Note the similarity between Fig. 3(a) and the density of states of the metallic glass. Both have a peak at $E \gtrsim 2$, and both vanish as E approaches 4. The polytope's density of states vanishes in the interval $3.708 \cdots < E \le 4$. In contrast, the fcc density of states is finite for all $-12 < E < 4$. A one-parameter family of eigenfunctions with $E = 4$ creates a divergence in the fcc density of states at $E = 4$.

Although we performed the analysis in Sec. II B for polytope 240, we can extend it to any tetracoordinated system which can be decomposed into two sublattices. Thus, Eq. (2.26) transforms all three densities of states in Fig. 3 into densities of states for H' and its crystalline and amorphous counterparts. We plot the density of states of H' in Fig. 4(a). The gap in the spectrum of H^s near $E = 4$ creates a gap in the spectrum of H' around $E = 0$. Sadoc and Mosseri[8] find a similar gap in the Connell-Temkin model. In contrast, the diamond lattice density of states[14] vanishes at a single point.

Equation (2.15) yields the sp^3 density of state on polytope 240 [Fig. 4(b)]. Note the gaps within the valence and conduction bands. These gaps arise from the gap in Fig. 4(a). Such gaps do not exist in amorphous silicon.[30] The crystalline silicon density of states vanishes at isolated points.[14] Polytope 240 describes the structure factor of amorphous silicon poorly also.[31] We believe that polytope 240 models silicon poorly because it contains only even numbered rings, whereas successful models contain many odd numbered rings.[30]

Gallium arsenide strongly favors even numbered rings. Thus, we expect polytope 240 to be a better model of amorphous gallium arsenide than amorphous silicon. Indeed, valence and conduction band gap are observed[30] in amorphous GaAs. Unequal site energies of Ga and As

create gaps[14,15] in crystalline GaAs. Polytope 240 predicts a slightly increased gap width due to icosahedral order.

Dramatic effects of icosahedral order appear in transition-metal d bands. Recall that d orbitals form a
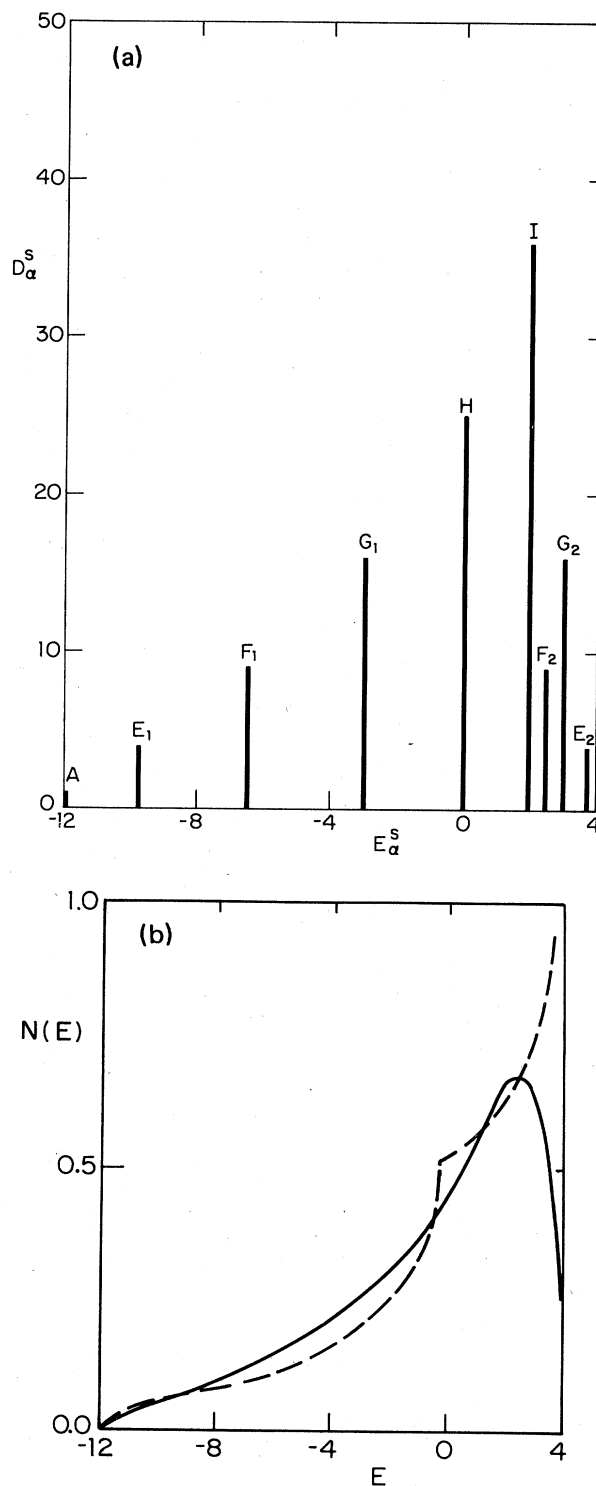

FIG. 3. s-band densities of states. (a) Polytope 120. (b) fcc crystal (dashed line) and dense random packing (solid line).

FIG. 5. Polytope 120 d band. We take $\sigma = -0.3563$ Ry, $\pi = 0.02091$ Ry, and $\delta = -0.0028$ Ry. Energies (2.48) are averaged over 0.03 Ry. Dashed lines show 70% and 90% filling of the band.
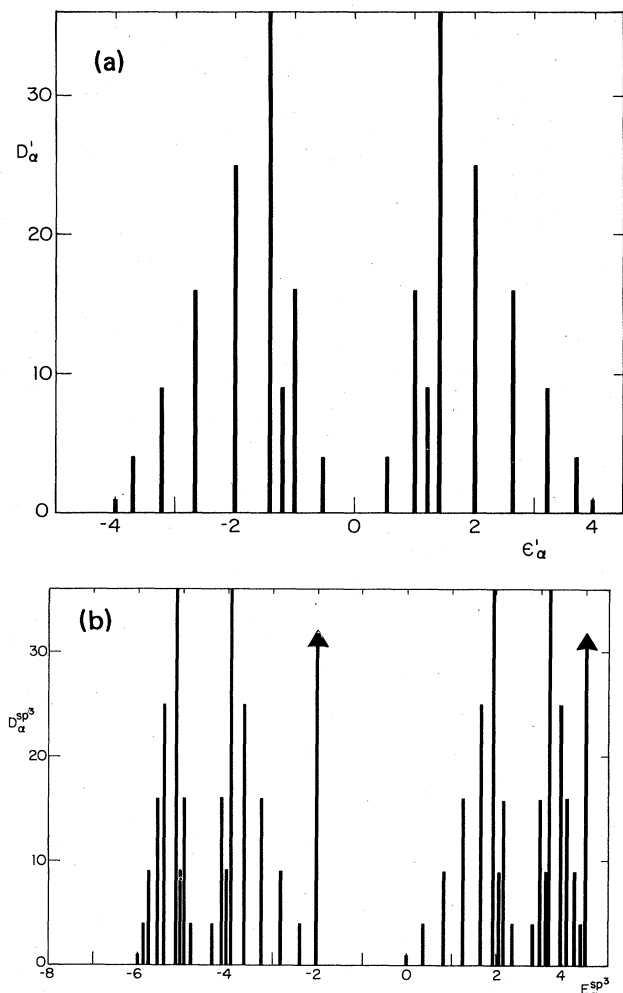

FIG. 4. Polytope 240 densities of states. (a) s band. (b) sp^3 hybrid orbitals. We take $V_1 = -1$ eV and $V_2 = -3$ eV.

basis for an irreducible representation of Y'. This prevents d level splitting at zero wave number. In contrast, the d band splits into blocks of degeneracy two and three at the center of the fcc Brillouin zone. In polytope 120 the d band remains degenerate at wave number $M = 1$ (see Table II).

We plot the d-band density of states in Fig. 5. The parameters σ, π, and δ are chosen to model nickel.[16,27,32] The values of σ, π, and δ are universal[32] up to an overall dilation of energy. Thus Fig. 5 qualitatively depicts the d-band density of states of both nickel and iron. Note the peak at band center. This is due to the absence of d level splitting in fields of icosahedral symmetry. Gaspard[29] observed a similar effect in a dense random packing model of glass.

It may be possible to measure the degree of icosahedral coordination experimentally. Dope the glass with atoms whose radius is comparable to nickel, but whose valence d electrons have a high ionization potential. These localized d electrons will be split according to their crystal field. The degree of splitting may be observable in photoemission fine structure.
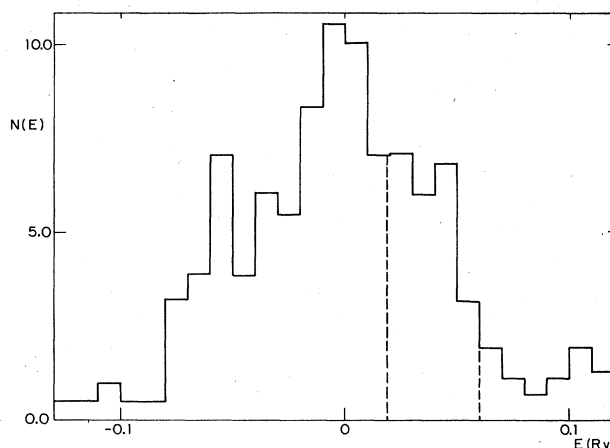
The shift in the transition metal density of states, from high energies in fcc crystals to the middle of the band in polytope 120, influences the magnetic properties of amorphous metals. Amorphous iron is ferromagnetic, whereas fcc iron is not. Face-centered-cubic nickel is ferromagnetic, whereas amorphous nickel is not. The Stoner criterion states that a material is ferromagnetic at low temperatures if

$$N(E_F)U_{\text{eff}} > 1 \ ,$$ (3.1)

where $N(E_F)$ is the density of states at the Fermi energy and U_{eff} is the effective Heisenberg exchange energy. Thus, increasing (decreasing) the density of states at the Fermi level increases (decreases) the probability of ferromagnetism.

The dashed lines in Fig. 5 show the Fermi energy for d^7 (iron) and d^9 (nickel) materials. Because the Fermi energy of iron is close to the band center, amorphous iron has a greater probability of ferromagnetism than fcc iron. Because the Fermi energy of nickel is close to a band edge, amorphous nickel has a lesser probability of ferromagnetism than fcc nickel. $N(E_F) = 5.8$ (atom Ry spin)$^{-1}$ in fcc nickel,[33] where $N(E_F) = 2.5$ (atom Ry spin)$^{-1}$ in polytope 120. Taking[32] $U_{\text{eff}} = 19$ atom Ry spin we find Eq. (3.1) satisfied for fcc nickel, but not polytope 120. Our polytope model of amorphous nickel correctly predicts magnetic trends.

ACKNOWLEDGMENTS

*Address after August 1985: Department of Physics, Carnegie-Mellon University, Pittsburgh, Pa. 15213.

[1]F. C. Frank and J. S. Kasper, Acta Crystallogr. **11**, 184 (1958); **12**, 483 (1959).

[2]H. S. M. Coxeter, *Introduction to Geometry* (Wiley, New York, 1969).

[3]D. R. Nelson, Phys. Rev. B **28**, 5515 (1983).

[4]P. Chaudhari and D. Turnbull, Science A **199**, 11 (1978).

[5]M. Hoare, Ann. N. Y. Acad. Sci. **279**, 168 (1978); see also I. S. Harris, R. S. Kidwell, and J. S. Northby, Phys. Rev. Lett. **53**, 2390 (1984).

[6]H. S. M. Coxeter, *Regular Polytopes* (Dover, New York, 1973).

[7]M. Kléman and J. F. Sadoc, J. Phys. (Paris) Lett. **40**, L569 (1979).

[8]J. F. Sadoc, J. Phys. (Paris) Colloq. **41**-C8 326 (1980), J. F. Sadoc and R. Mosseri, Philos. Mag. B **45**, 467 (1982).

[9]D. P. DiVincenzo, R. Mosseri, M. H. Brodsly, J. F. Sadoc, Phys. Rev. B **29**, 5934 (1984); M. H. Brodsky and D. P. DiVincenzo, Physica **117B/118B** 971 (1983).

[10]D. R. Nelson and M. Widom, Nucl. Phys. B **240**, 113 (1984).

[11]S. Sachdev and D. R. Nelson, Phys. Rev. Lett. **53**, 1947 (1984).

[12]M. Widom, in *Proceedings of the Thirteenth International Colloquium on Group Theoretical Methods in Physics* (World Scientific, Singapore, 1984), p. 348.

[13]D. L. Weaire and M. F. Thorpe, Phys. Rev. B **4**, 2508 (1971).

[14]M. F. Thorpe and D. L. Weaire, Phys. Rev. B **4**, 3518 (1971).

[15]J. P. Straley, Phys. Rev. B **6**, 4086 (1972).

[16]J. C. Slater and G. F. Koster, Phys. Rev. **94**, 1498 (1954).

[17]J. P. Sethna, Phys. Rev. Lett. **51**, 2198 (1983).

[18]G. Bergman, J. L. T. Waugh, and L. Pauling, Acta Crystallogr. **10**, 254 (1957).

[19]P. DuVal, *Homographies, Quaternions, and Rotations* (Oxford, London, 1964).

[20]A. G. McLellan, J. Chem. Phys. **34**, 1350 (1961); P. H. Butler, *Point Group Symmetry Applications* (Plenum, New York, 1981); D. R. Pooler, J. Phys. A **13**, 1197 (1980).

[21]J. Raynal, J. Math. Phys. **25**, 1187 (1984).

[22]T. Damhus, S. E. Harnung, C. E. Schäffer, Theor. Chim. Acta **65**, 433 (1984).

[23]L. D. Landau and E. M. Lifshitz, *Quantum Mechanics,* 3rd ed. (Pergamon, New York, 1977).

[24]M. Bander and C. Itzykson, Rev. Mod. Phys. **38**, 330 (1966).

[25]N. P. Warner, Proc. R. Soc. London Ser. A **383**, 359 (1982).

[26]R. Mosseri and J. F. Sadoc (unpublished).

[27]G. C. Fletcher, Proc. Phys. Soc. London Ser. A **65**, 192 (1952).

[28]R. J. Jelitto, J. Phys. Chem. Solids. **30**, 609 (1969).

[29]J. P. Gaspard, in *Structure and Excitation of Amorphous Solids (Williamsburg, Va., 1976),* Proceedings of an International Conference Structure and Excitation of Amorphous Solids, edited by G. Lucovsky and F. L. Galeener (AIP, New York, 1976), p. 372.

[30]J. D. Joannopoulos and M. L. Cohen, *Solid State Physics* (Academic, New York, 1976), Vol. 31, p. 71.

[31]S. Sachdev (private communication).

[32]H. Ehrenreich and L. Hodges, in *Methods in Computational Physics* (Academic, New York, 1968), Vol. 8, p. 149.

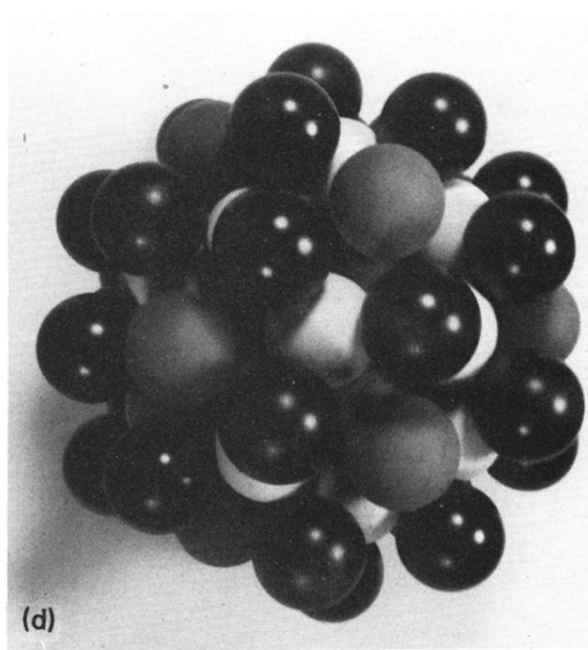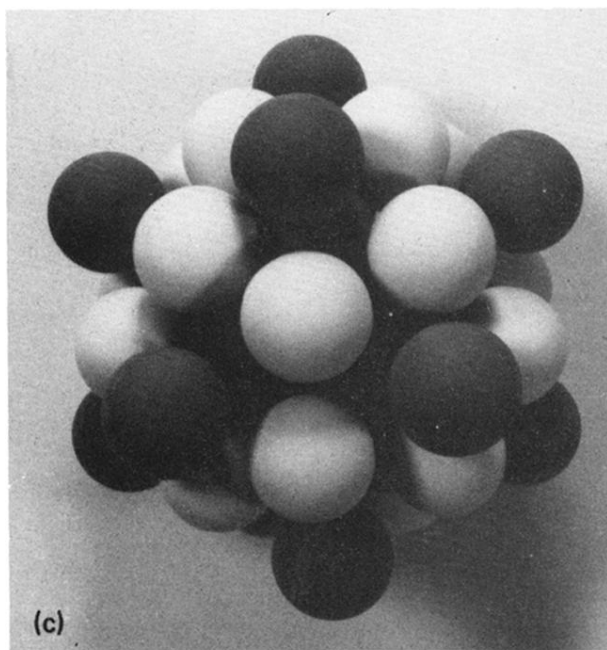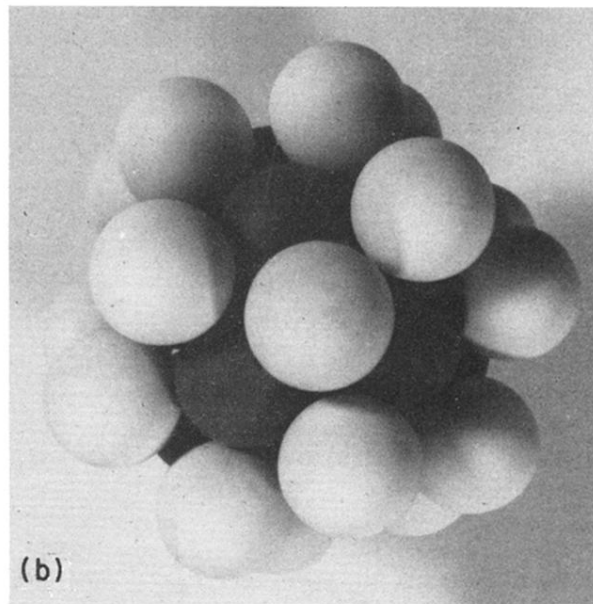[33]L. Hodges, H. Ehrenreich, and N. D. Lang, Phys. Rev. **152**, 505 (1966).
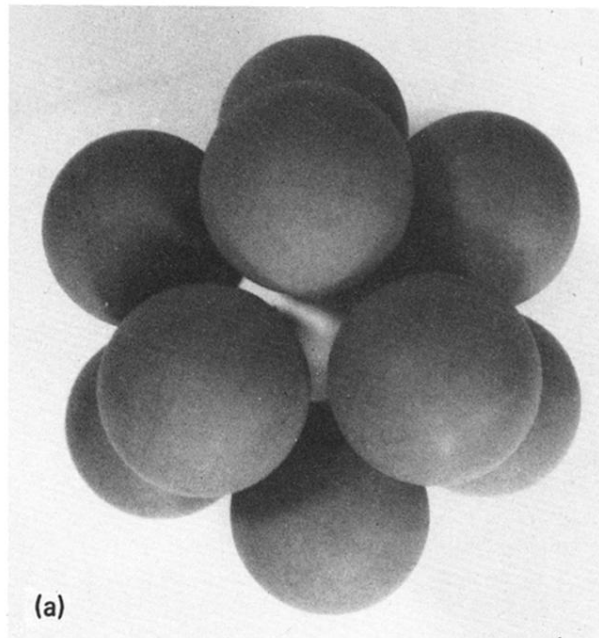
FIG. 1. Fragments of polytope 120 in R^3. (a) Coordination shell V_1 forms an icosahedron. (b) Coordination shell F_2 forms a dodecahedron. (c) Coordination shell V_3 forms an icosahedron. (d) Coordination shell E_4 forms an icosidodecahedron.